

Infrared antennas coupled to lithographic Fresnel zone plate lenses

Francisco Javier González, Javier Alda, Bojan Ilic, and Glenn D. Boreman

Several designs for Fresnel zone plate lenses (FZPLs) to be used in conjunction with antenna-coupled infrared detectors have been fabricated and tested. The designs comprise square and circular FZPLs with different numbers of Fresnel zones working in transmissive or reflective modes designed to focus infrared energy on a square-spiral antenna connected to a microbolometer. A $163\times$ maximum increase in response was obtained from a 15-zone circular FZPL in the transmissive mode. Sensor measurements of normalized detectivity D^* resulted in a $2.67\times$ increase with FZPLs compared with measurements made of square-spiral antennas without FZPLs. The experimental results are discussed and compared with values obtained from theoretical calculations. © 2004 Optical Society of America

OCIS codes: 040.3060, 230.3990.

1. Introduction

The use of antenna-coupled infrared detectors has found applications in several fields of science and technology.^{1–6} Infrared antennas have proved to be an effective solution when polarization sensitivity, tunability, directionality, point-detector characteristics, and room-temperature operation are necessary.

Individual infrared antennas have a typical collection aperture sizes of the order of λ^2 ; therefore the amount of energy that they can collect is quite small.^{7,8} There are several approaches to increasing the collected energy, such as illuminating from the substrate, modifying the fabrication materials, and adding collection optics.^{9,10} To use infrared antennas in imaging systems, which have typical pitch sizes of $20\ \mu\text{m} \times 20\ \mu\text{m}$ to $50\ \mu\text{m} \times 50\ \mu\text{m}$ two-dimensional arrays have been fabricated.⁶ The problem with these types of detector is that adding

elements in series to cover a bigger area will increase the total noise of the detector. To keep the noise low, i.e., at the level of a single-element microbolometer, but still have a large collection area, we fabricated Fresnel zone plate lenses (FZPLs) to collect infrared energy and focus it onto a single antenna-coupled microbolometer. FZPLs are practical energy collectors, which are already in use in the microwave and millimeter spectrum, that we investigate in this paper at infrared frequencies.^{11–14} FZPLs are well suited for integration with infrared antennas. They are planar structures that can be fabricated with the same lithographic tools used for fabricating antenna-coupled detectors.

In this paper we describe using the collecting properties of FZPLs to concentrate the optical flux that reaches an infrared antenna. The increase in irradiance is followed by an increase in the signal produced by the detector. In this paper we demonstrate how a custom FZPL is able to enhance the responses of infrared antennas. In Section 2 we show the design parameters for circular- and square-shaped FZPLs. We also include the definition of a figure of merit that is the gain in response of an infrared antenna with the FZPL compared with a single antenna without a FZPL. Section 3 is devoted to a description of the fabrication process and to explaining the characteristics of the FZPLs and their associated infrared antennas. In Section 4 we show how the characterization of these devices was made and the experimental results were obtained from this characterization. In that section we also compare these experimental results with those obtained from simu-

F. J. González is with the Instituto de Investigación en Comunicación Óptica, Universidad Autónoma de San Luis Potosí, Alvaro Obregón 64, San Luis Potosí, Mexico. J. Alda (j.alda@fis.ucm.es) is with School of Optics, University Complutense of Madrid, Avenida Arcos de Jalón s/n, 28037 Madrid, Spain. B. Ilic is with Cornell NanoScale Science & Technology Facility, 250 Duffield Hall, Cornell University, Ithaca, New York 14853-2000. G. D. Boreman is with School of Optics—Center for Research and Education in Optics and Lasers, University of Central Florida, 4000 Central Florida Boulevard, Orlando, Florida 32816-2700.

Received 3 May 2004; revised manuscript received 17 August 2004; accepted 20 August 2004.

0003-6935/04/336067-07\$15.00/0

© 2004 Optical Society of America

lations for which the actual parameters of the FZPLs were used. The theoretical results are also displayed to enable us to determine the optimum theoretical improvement in the detected signal. Finally, in Section 5 we summarize the main conclusions of this paper.

2. Fresnel Zone Plate Lenses

The principle of operation of FZPLs is based on the wave nature of light. The wave front arriving at the FZPL is divided into portions, or zones. The criteria used to define these zones are well defined in the literature.^{14,15} The zones of the FZPL described in this paper are designed to focus an incident plane wave at an infrared antenna that is a distance of 380 μm away from the FZPL. The medium between the FZPL and the infrared antenna is silicon, and the focal distance is given by the thickness of the silicon wafer ($\sim 380 \mu\text{m}$).

The electric field at the infrared antenna plane is given by the following equation:

$$E_{\text{ant}}(x, y) = \iint E(x', y') F(x', y') \times K(x, y, x', y') dx' dy', \quad (1)$$

where $E(x', y')$ is the electric field distribution at the plane of the FZPL, $F(x', y')$ is a function related to the FZPL that provides the spatial distribution in transmission or reflection of the FZPL, and $K(x, y, x', y')$ is a function that contains all the information about the optical path between a given point on the FZPL and another point on the infrared antenna plane. This function is given as follows:

$$K(x, y, x', y') = \frac{1}{2} \left[1 + \frac{d_0}{d(x, y, x', y')} \right] \times \frac{1}{d(x, y, x', y')} \times \exp \left[-i2\pi \frac{nd(x, y, x', y')}{\lambda_0} \right], \quad (2)$$

where d_0 is the distance between the plane of the FZPL and the plane of the infrared antenna, n is the index of refraction of the medium between these planes, λ_0 is the wavelength of the optical radiation in vacuum, and $d(x, y, x', y')$ is the distance between any given point in the FZPL plane characterized by its coordinates (x', y') and another point at the infrared antenna plane characterized by (x, y) . The term inside the first set of brackets and the $\frac{1}{2}$ factor is also known as the obliquity factor. Distance d is given as

$$d(x, y, x', y') = [d_0^2 + (x - x')^2 + (y - y')^2]^{1/2}. \quad (3)$$

With respect to $K(x, y, x', y') = K(x - x', y - y')$, the integral of Eq. (1) can be seen as a convolution product between the electric field just after the FZPL and the function that describes the propagation from the FZPL to the plane of interest. By using these equa-

tions it is possible to obtain a map of the electric field at any given point about the principal focus of the FZPL. In this paper we are interested mainly in the value at the location of the infrared antenna. The focusing of the incoming radiation by the FZPL will produce an increase in irradiance and a higher response than that obtained without the FZPL.

The FZPL is characterized by the sizes of the successive zones. We are interested in FZPLs that are able to focus the incoming radiation onto a reduced area on the detection plane where the antenna is placed. Therefore the focal point of the FZPL should be located on the infrared antenna. The plane of the FZPL and the plane where the antenna is located are parallel. With this arrangement the radii of the boundaries of the circular Fresnel zones are given by

$$r_m = \left(md_0 \frac{\lambda_0}{n} \right)^{1/2}, \quad (4)$$

where d_0 is the focal length of the FZPL (which coincides with the thickness of the wafer), n is the index of refraction of the wafer, and m is the order of the Fresnel zone.

Although symmetry defines the Fresnel zones as circular, for some applications it could be useful to have rectangular or square FZPLs. For example, square FZPLs are better suited to the intrinsic geometry of an array of rectangular pixels. Square FZPLs are also considered in this paper. These square Fresnel zones are designed to have the same areas as the corresponding circular zones. The relation between half of the side of the square and the radius of a circular zone of the same order is

$$x_i = \frac{r_i \sqrt{\pi}}{2} = 0.8862 r_i. \quad (5)$$

Once the geometry of the FZPL is set, the mode of operation of the FZPLs has to be determined. We have distinguished two modes: reflective and transmissive. In the transmissive mode the light is incident upon the side of the wafer where the FZPL is located and reaches the infrared antenna from the substrate side. In the reflective mode the light is incident on the surface where the antenna is located, propagates to the FZPL, and is reflected back to the infrared antenna, incident from the substrate side too. The FZPL works differently for these two modes. In the transmissive mode the transmittance is zero in the zones where the metal is deposited and is equal to the transmissivity between air and substrate in the rest of the zones. In the reflective mode the reflectance is ~ 1 for those zones where the metal is deposited, and it is equal to the reflectance of the substrate-air interface for the other zones. The phase shift in the reflection is also taken into account when the $F(x', y')$ function that describes the FZPL is

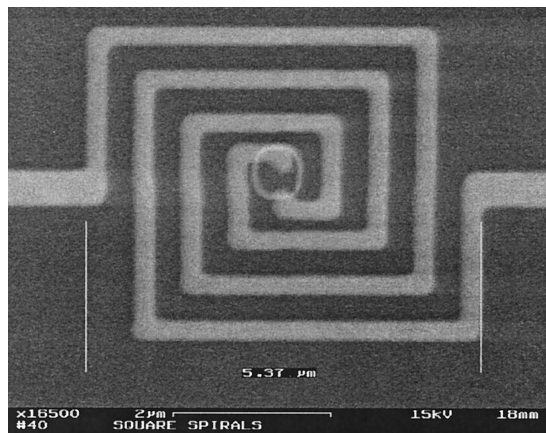


Fig. 1. Electron-microscope photograph of the optical spiral antenna used in this study. The shape of the spiral antenna should not be confused with the square FZPL written on the other side of the wafer.

computed. The associated transmission and reflection coefficients in amplitude are

$$t = \frac{2n}{n + n'}, \quad r = \frac{n - n'}{n + n'}, \quad (6)$$

respectively, where n and n' are the indices of refraction of the incident and refracted media.

An objective of this paper is to provide a figure of merit to describe the effect of inclusion of a FZPL. This figure of merit is defined as a gain factor (GF) evaluated at the location of the infrared antenna:

$$GF = \frac{\text{Irradiance with the FZPL}}{\text{Irradiance without the FZPL}}. \quad (7)$$

In Section 4 below, this figure of merit is calculated for the types of device fabricated. The theoretical expectations for this value are compared with the experimental values of the signals obtained from the antennas. The signal is proportional to the incident irradiance. The antennas with or without FZPLs are equal in design and fabrication. Their only difference is that some of them have a FZPL properly aligned at the back side of the wafer. Therefore the ratio between signals is a measurement of the GF. The results are analyzed in Section 4.

3. Electron-Beam Lithography of FZPLs Integrated with Infrared Antennas

Square-spiral-antenna-coupled niobium microbolometers (Fig. 1) were used as detectors for this study; these detectors were fabricated by electron-beam lithography and liftoff on 380- μm silicon wafers with 200 nm of thermally grown SiO_2 for thermal and electrical isolation.¹⁶ The physical size of these detectors was approximately 5 μm \times 5 μm . The antenna elements were made from 100 nm of evaporated gold, and the microbolometer was a 500 nm \times 500 nm niobium patch that was 60 nm thick and was located at the feed of the antenna.

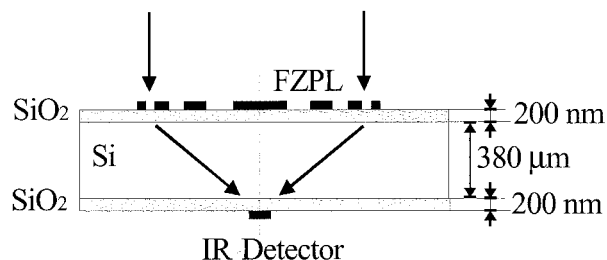


Fig. 2. FZPL in the transmissive configuration coupled to an antenna-coupled microbolometer.

The FZPLs were patterned by use of optical lithography and aligned to a single-element square-spiral-antenna-coupled microbolometer on the back side of the wafer by an Electronic Visions backside aligner, model EV620. The FZPL lenses were made from 100 nm of electron-beam evaporated gold over a 5-nm layer of chrome used as an adhesion layer. The configuration of the FZPL and the infrared antenna is depicted in Fig. 2. The FZPL is intended to work on axis at a wavelength of 10.6 μm . At this wavelength the silicon wafer is transparent, showing index of refraction $n = 3.42$. The focal length of the FZPL can be established at $f' = 380 \mu\text{m}$. The optical axis is perpendicular to the wafer's surface and intersects the location of the infrared antenna. We obtain the limits of the zones by following the relation given in Eq. (4) and substituting $d_0 = 380 \mu\text{m}$. The numerical values that describe the sizes of the circular and square FZPLs are presented in columns 2 and 4 Table 1. By substituting the values of the index of refraction of the materials involved in the fabrication of the FZPL into Eqs. (6) we obtained the transmission and

Table 1. Dimensions of the Zones for Circular and Square Geometries and for the Conditions of Fabrication Given by the Wafer Dimensions and Materials^a

Zone Number, i	Circular FZPL: Limiting Radius r_i (μm)		Square FZPL: Limiting Half-Side x_i (μm)	
	Calculated	Fabricated	Calculated	Fabricated
1	32.930	34.1	30.408	30.9
2	46.569	46.6	43.003	42.3
3	57.036	59.2	52.667	52.8
4	65.859	66.1	60.815	59.9
5	73.633	75.8	67.993	68.1
6	80.661	81.5	74.483	73.2
7	87.123	89.6	80.451	80.6
8	93.140	94.9	86.006	84.6
9	98.790	101.8	91.223	90.8
10	104.134	105.9		
11	109.217	111.5		
12	114.073	115.5		
13	118.731	122.0		
14	123.213	125.3		
15	127.537	130.6		

^aThe columns headed Calculated were obtained from the theoretical prediction; those headed Fabricated show the values measured on the fabricated FZPLs.

Table 2. Coefficients of Transmission and Reflection for the Alternate Zones Involved in the Fabricated FZPL

Type of Zone	Coefficient	
	t	r
Deposited zone (metal-wafer)	0	$0.9834 \exp(i3.0432)$
Blank zone (air-wafer)	0.4523	0.5477

reflection coefficients applied in the calculation (see Table 2). When the effect of the SiO₂ thin layer is taken into account the change in the value of the modulus of these coefficients is negligible.

Two different types of FZPL were fabricated: the traditional ones, which consist of concentric rings (Fig. 3, top) and an approximation of these made by use of concentric squares (Fig. 3, bottom). Eight circular and five square FZPLs were fabricated. These lenses vary in the number of zones that each one has:

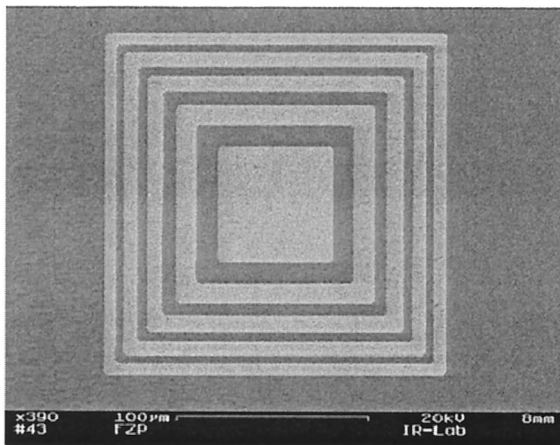
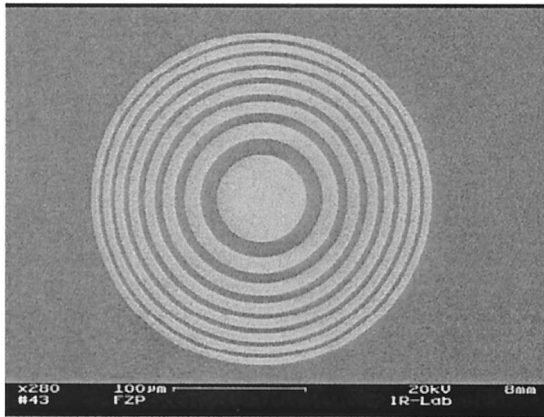


Fig. 3. Electron-microscope photographs of two FZPLs. At the top we present a circular FZPL with eight metalized Fresnel zones; it belongs to a series of circular FZPLs with increasing numbers of metalized zones. At the bottom we show a squared FZPL with five metalized Fresnel zones; it belongs to a series of square FZPLs with increasing numbers of metalized zones.

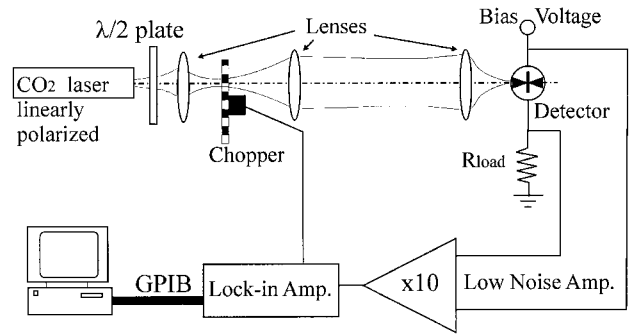


Fig. 4. Schematic of the experimental setup used to test the infrared antenna's response. GPIB, general purpose interface bus.

Circular FZPLs have one to eight opaque zones, whereas square FZPLs have one to five opaque zones.

The main functions of the zone plate are to increase the gain of the spiral antenna and also to reduce the energy loss that is due to guided waves in the substrate by altering the boundary conditions of the dielectric slab waveguide.¹²

4. Testing Procedure and Results

The test setup that we used to characterize these FZPL-coupled detectors is shown in Fig. 4. A CO₂ laser emitting infrared radiation at 10.6 μm focused by an $f/8$ optical train was used. The diameter of the beam spot that encloses 84% of the total flux is approximately 200 μm; the power at the focal plane was set by use of a wire-grid polarizer to 33 mW, which gives an approximate irradiance of 88 W/cm² at the focus.

The FZPL-coupled detectors were tested in the transmissive configuration (as shown in Fig. 2) and in a reflective configuration, in which the radiation comes through the detector plane first and then reflects off the FZPL.

After fabricating the FZPLs we measured the actual sizes of the Fresnel zones (the measured values are given in columns 3 and 5 of Table 1). Because of overexposure during the fabrication process the zones containing the metal deposition were a little wider than predicted. For example, the metalized zones of the squared FZPL shown in Fig. 3 had the following widths (in micrometers): 30.9, 10.5, 8.2, 7.4, and 6.2 (the expected values were 30.4, 9.7, 7.2, 6.0, and 5.2 μm, respectively). We analyzed four configurations, combining the transmissive and reflective modes of operation and the circular and square geometry of the alternate zones. At the same time we calculated the expected GFs for these four configurations, using the model of operation of the FZPL described in Section 2. We made the calculations by simulating a Gaussian beam that had the same size as the probe beam and by using a uniform plane-wave model. We achieved a last refinement of the calculation by considering the actual sizes of the zones written on the substrate (listed in columns 3 and 5 of Table 1). In Fig. 5 we have plotted the GFs experimentally obtained for several configurations

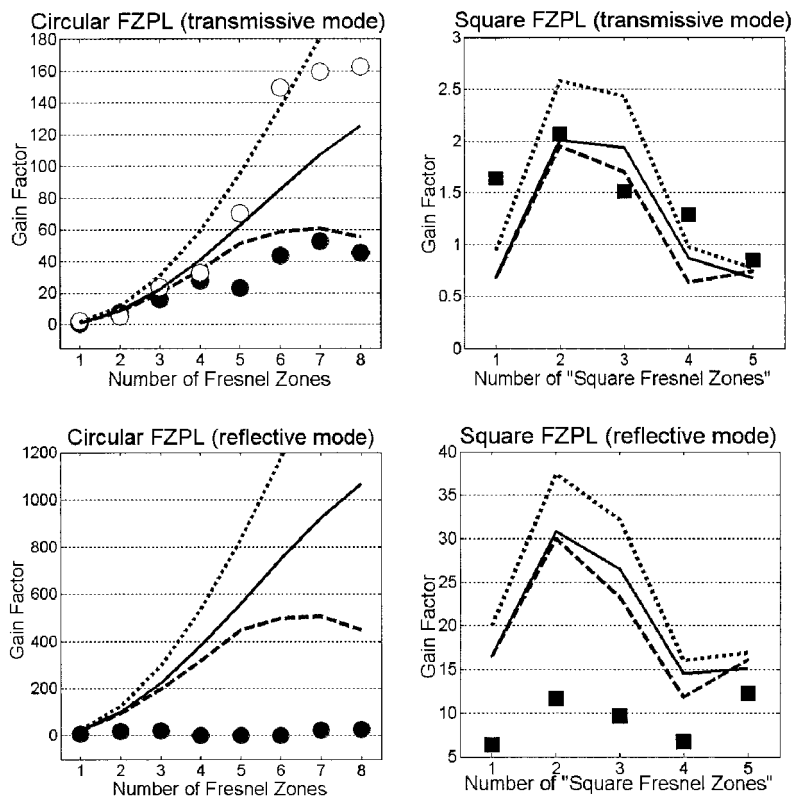


Fig. 5. GF of the FZPLs fabricated with various numbers of zones for the two modes of operation (transmissive and reflective) and the two geometries: circular (circles) and square (squares). Dotted curves, input beams with uniform amplitude; the sizes of the zones are the theoretical sizes. Solid curves, results of modeling a Gaussian that corresponds to the probe beam. The zones are still dimensioned with the theoretical values. Dashed curves, simulation of a Gaussian beam incident upon a FZPL for which the dimensions of the Fresnel zones are those actually fabricated and measured. In the figure for the circular transmissive mode we have included two series of data that belong to different series of devices. The GF, represented by filled symbols, is for those devices precisely measured to include the actual dimensions of the zones into the calculations.

and for a set of FZPLs with several numbers of zones. In this figure we have also included the results obtained after the effects of the FZPLs were simulated.

Several consequences may follow from these results. The GF is larger than 1 for all the devices except a square FZPL with five zones and a circular FZPL with only one zone. The maximum measured value of the GF was 163 measured on a circular FZPL working in transmissive mode and having 15 Fresnel zones (8 circles filled with gold). The maximum theoretical GF for the same conditions of operation and geometry is 221. The difference between the measured and theoretical values is due to nonideal effects such as the nonuniformity of the laser beam used to make the measurements and the difference in dimensions of the FZPL owing to fabrication issues. First we found a higher response for circular FZPLs than for square FZPLs. In addition, whereas circular FZPLs have larger GFs for an increase in the number of zones, the square version does not follow this trend. This is so because, when one is considering square zones farther apart from the center, their coincidence with the actual Fresnel zones becomes increasingly worse. A second result of this study is that the transmissive operation fits better with the theoretical expectations than with the reflective mode. The ex-

perimental results are better modeled when the actual sizes of the Fresnel zones are included in the calculation along with the dimensions of the Gaussian probe beam. Although the magnitudes of the expected and the experimental GFs for the reflective mode are different, the trend in the variation of the experimental GF is the same, especially for the square FZPL. The discrepancy in the values is due to the fact that, before arriving at the FZPL plane, the laser beam needs to cross the plane where the infrared antennas are written. This plane is full of obstacles in the form of opaque bond pads and connection lines. These obstacles obscure the light path and reduce the actual irradiance arriving at the FZPL by a considerable amount. This obscuration effect diminishes the signal and the corresponding GF.

A result that summarizes the finding of this paper is the calculation of normalized detectivity D^* for circular FZPLs in the transmissive mode. D^* is defined as the rms signal-to-noise ratio in a 1-Hz bandwidth per unit rms incident radiant power per square root of detector area. The importance of D^* comes from the fact that it permits comparison of detectors of the same type but with different areas and different measurement bandwidths. Increasing the num-

Table 3. Values of the Ratio of D^* for Two Series of Identical Infrared Antennas Attached with Circular FZPLs with Different Numbers of Opaque Zones and Working in Transmissive Mode and for Those Infrared Antennas without the FZPL

Number of Opaque Zones	Ratio of D^*
1	0.15
2	0.18
3	0.62
4	0.73
5	1.38
6	2.67
7	2.61
8	2.49

ber of Fresnel zones increases the response of the detector. However, the collection area of the detector, which is the area covered by the largest zone plate, also increases. In Table 3 we present the value of the ratio of the calculated D^* for the FZPL-coupled detector and a detector without a FZPL. From these results we can see that we get an increase in D^* after the fifth opaque zone, which is $\sim 200 \mu\text{m}$ in diameter. From our experimental results, the maximum gain in D^* is 2.67, and it appears for a circular FZPL with six opaque zones working in transmissive mode.

5. Conclusions

The use of FZPLs to improve the response and detectivity of antenna-coupled infrared detectors has been demonstrated theoretically and experimentally. The FZPLs were designed with circular and square zones. We designed the square FZPLs by maintaining the area of their corresponding circular Fresnel zones. The FZPLs were written on the back side of a silicon wafer. The focus is located at the infrared antenna position. The FZPL can operate in a transmissive mode and in a reflective mode. The calculation for the irradiance at the focus of the FZPL has taken into account the indices of the materials used and the phase shifts that occur at the interfaces. A figure of merit for evaluating the effect of the FZPL is defined as the ratio between the irradiance on the location of the infrared antenna with an FZPL and the irradiance without the FZPL. After fabricating the different designs we measured the response of the antenna-coupled detectors.

The results for the reflective mode do not agree with the expected values. This is so because of the obscuration produced by the connection patches and lines written about the antenna. They diminish the amount of radiation that actually reaches the FZPL and is able to focus on the antenna. The expected theoretical GF reached values near 1000 for reflective FZPLs. Although this value for GF was not obtained, the circular FZPL operated in reflective mode provided experimental values of GF of ~ 20 . The square FZPLs behave worse than the circular, as predicted by the theoretical model.

The response of the detectors increases as predicted by the theoretical model for the transmissive mode. For circular FZPLs operating in this mode we corrected the theoretical expectations by introducing the actual values of the sizes of the circular zones. After this correction the experimental data showed good agreement. The maximum experimental value for the gain factor was $163\times$ for a circular FZPL with eight opaque zones operating in transmissive mode. An optimization of the fabrication process may increase the GF above 200 for a FZPL with eight opaque zones working in transmissive mode. This optimization should reduce the difference between the expected (theoretical) and fabricated dimensions of the Fresnel zones. In our devices, D^* also showed a maximum increase of a factor of $2.67\times$.

Summarizing, FZPLs have been proved to be valuable elements for improving the performance of infrared antennas.

This research was performed in part at the Cornell Nanofabrication Facility (a member of the National Nanofabrication Users Network), which is supported by the National Science Foundation under grant ECS-9731293, its users, Cornell University, and Industrial Affiliates. This material is based on research supported by NASA grant NAG5-10308. This research has been partially supported by research project TIC2001-1259 of the Ministerio de Ciencia y Tecnología of Spain.

References

1. I. Wilke, W. Herrmann, and F. Kneubühl, "Integrated nanostrip dipole antennas for coherent 30 THz infrared radiation," *Appl. Phys. Lett.* **71**, 1607-1609 (1997).
2. G. Boreman, C. Fumeaux, W. Herrmann, F. Kneubühl, and H. Rothuizen, "Tunable polarization response of planar asymmetric-spiral infrared antennas," *Opt. Lett.* **23**, 1912-1914 (1998).
3. I. Codreanu, C. Fumeaux, D. Spencer, and G. Boreman, "Microstrip antenna-coupled infrared detector," *Electron. Lett.* **35**, 2166-2167 (1999).
4. W. A. Beck and M. S. Mirotznik, "Microstrip antenna coupling for quantum-well infrared photodetectors," *Infrared Phys. Technol.* **42**, 189-198 (2001).
5. K. B. Crozier, A. Sundaramurthy, G. S. Kino, and C. F. Quate, "Optical antennas: resonators for local field enhancement," *J. Appl. Phys.* **94**, 4632-4642 (2003).
6. F. J. Gonzalez, M. A. Gritz, C. Fumeaux, and G. D. Boreman, "Two dimensional array of antenna-coupled microbolometers," *Int. J. Infrared Millim. Waves* **23-25**, 785-797 (2002).
7. C. Fumeaux, G. Boreman, W. Herrmann, F. Kneubühl, and H. Rothuizen, "Spatial impulse response of lithographic infrared antennas," *Appl. Opt.* **38**, 37-46 (1999).
8. J. Alda, C. Fumeaux, I. Codreanu, J. Schaefer, and G. Boreman, "A deconvolution method for two-dimensional spatial-response mapping of lithographic infrared antennas," *Appl. Opt.* **38**, 3993-4000 (1999).
9. J. Alda, C. Fumeaux, M. Gritz, D. Spencer, and G. Boreman, "Responsivity of infrared antenna-coupled microbolometers for air-side and substrate-side illumination," *Infrared Phys. Technol.* **41**, 1-9 (2000).
10. I. Codreanu and G. Boreman, "Influence of a dielectric sub-

- strate on the responsivity of microstrip dipole-antenna-coupled infrared microbolometers," *Appl. Opt.* **41**, 1835–1840 (2002).
11. J. C. Wiltse and J. E. Garrett, "The Fresnel zone plate antenna," *Microwave J.* **34**, 101–114 (1991).
 12. M. A. Gouker and G. S. Smith, "A millimeter-wave integrated-circuit antenna based on the Fresnel zone plate," *IEEE Trans. Microwave Theory Techn.* **40**, 968–977 (1992).
 13. G. Z. Jiang and W. X. Zhang, "Theoretical and experimental studies of the Fresnel zone plate lens antenna," *Electromagnetics* **19**, 385–399 (1999).
 14. H. D. Hristov, *Fresnel Zones in Wireless Links, Zone Plate Lenses and Antennas* (Artech House, Norwood, Mass., 2000).
 15. E. Hecht, *Optics* (Addison-Wesley, Reading, Mass., 1998).
 16. C. Fumeaux, M. A. Gritz, I. Codreanu, W. L. Schaich, F. J. González, and G. D. Boreman, "Measurement of the resonant lengths of infrared dipole antennas," *Infrared Phys. Technol.* **41**, 271–281 (2000).